PROBLEMS OF 3D RECONSTRUCTION AND VISUALISATION IN EIT

MARCIN KOCIKOWSKI, ARTUR POLIŃSKI,
ANTONI NOWAKOWSKI, JERZY WTOREK

Department of Medical and Ecological Electronics, Faculty of Electronics, Telecommunications & Informatics, Technical University of Gdansk, Narutowicza 11/12, 80-952 Gdansk, Poland

Abstract: In the paper different algorithms of electroimpedance tomography (EIT) are presented. The properties of EIT are discussed. Problems of proper modelling of measurement electrodes are introduced. Results obtained from developed 3D reconstruction algorithm are presented. For practical reasons the number of measurement electrodes should be increased. Measurement errors should be small, to avoid amplifying them by reconstruction algorithm. Assumed conductivity distribution for the first iteration should be as close to the real one as possible. Reconstruction time (of absolute value of conductivity) is still a problem for practical applications.

1. Introduction

Electrical impedance tomography reconstructs a conductivity (resistivity) distribution in an examined object basing on electrical measurements made on the boundary of this object. Depending on the method the currents or voltages are measured. The main drawback of this method is its relatively low resolution and low sensitivity in the centre of the examined object. The second problem is time needed for reconstruction if absolute value of conductivity distribution should be obtained. Comparing traditional computer tomography and EIT, the last one has some advantages — it is non-invasive, allows continuos monitoring of biological processes, is using electrical signal instead of ionising radiation and allows to construct low cost and portable devices. Poor resolution and low sensitivity in the central region of the examined object and long reconstruction time (in some cases) limit possible applications. Because of that some effort is put to increase the quality of reconstructed images and to speed up the process of reconstruction. Stability of an algorithm is also very important. Especially when the absolute value of conductivity in an examined object is reconstructed, the algorithm should converge to the real value, even if assumed conductivity distribution inthe first iteration differs significantly from the real one. It should also not be sensitive for measurement errors.

One possibility to improve resolution is to increase the number of electrodes. The higher number of electrodes the better resolution and sensitivity of measurements may be achieved. Yet, with the increase of the number of electrodes,

the problem of measurement noise increases (the difference between measured values in neighbouring electrodes have to be greater than the value of measurement noise). Typically, the number of driving and measuring electrodes varies from 16 to 128 or even more in different hardware solutions [1]. The number of electrodes is also limited by their size. Bigger electrodes take more space and because of this less electrodes can be put, which means lower resolution. The advantage of using large electrodes is the small value of their impedance. Their drawback is averaging of signal from part of surface. The drawback of small electrodes is their big value of impedance, which causes measurement problems.

The sensitivity of measurements is a function of distance from the measurement ports. Near the boundary of the examined object it can be a thousand times greater than in the centre of this object. Therefore it is very important to propose methods of measurements and reconstruction algorithms of increased sensitivity inside the body or with more uniform distribution of the sensitivity function. Rather poor sensitivity distribution is due to ill-conditioning — the important problem in reconstruction (big conductivity variation inside examined object may result in low data variation on the surface). Because of that reconstruction algorithms use, openly or not, so called regularization techniques. These all factors limit the quality of reconstructed images and especially their spatial resolution.

Another problem is the complexity of computation. Most algorithms are based on Finite Element Method (FEM) and Boundary Element Method (BEM). We will focus on FEM and limitation of algorithms which use this method. The available computer memory is limiting the number of elements in a model. Increase in the number of elements (which is equivalent to an increase in memory consumption) may cause the use of a swap file during reconstruction, which slows it down. Using the same model (the same number of elements) different algorithms need different time to obtain a reconstructed image. It is due to the way, which was used, when algorithm was invented.

It should also be mentioned that the inverse problem is nonlinear. If linear dependence between conductivity distribution and measured voltages (or currents) on the surface is assumed, then it is possible to obtain very fast and simple reconstruction algorithms, but the quality of images is rather poor (might be good when conductivity changes are small). Because of that the reconstruction algorithms can be divided into two groups. The first group concerns the reconstruction of the relative conductivity, while the second — the absolute values. In the first group the linearity between measurements and conductivity distribution is assumed (additionally also that the conductivity distribution is uniform or close to that obtained from the previous measurement). The advantage of this method is that reconstruction algorithms are simple and very fast, which allows to obtain 2D moving images in real time. The main disadvantage is low accuracy of reconstruction. The second group of algorithms allows to obtain more realistic reconstruction but calculation cost is much greater. The new algorithm presented in this paper, representing second group, was

proposed by M. Kocikowski and was a part of his Ph.D. thesis [2]. It should also be mentioned that iterative use of most of algorithms of the first group allows to reconstruct an absolute value of conductivity, while using one iteration in the second group allows reconstruction of the changes of conductivity.

2. Reconstruction algorithms

Most important algorithms, used for reconstruction of absolute conductivity values, are presented. Algorithms which allow to reconstruct conductivity changes are omitted, but as it was mentioned, in most cases one iteration of presented algorithms can be used to obtain changes of conductivity.

1° — Backprojection

This method is based on back projection used in roentgen tomography. For each excitation the examined object is divided into subregions by equipotential lines ending on measurement electrodes [3,4]. The new value of resistivity for that excitation is calculated from the formula:

$$\rho_i^n = \rho_i^{n-1} \frac{u_m}{u_c},$$

where: ρ_i^n — resistivity of element i-th after n correction, ρ_i^{n-1} — resistivity of element i-th after n-1 correction, u_m — measured voltage, u_c — calculated voltage. As it can be seen from the above formula for each of subregions the resistivity is granted, which value is proportional to the ratio of two voltages. The first voltage is measured while the second one is obtained from simulations study. The new value of resistivity of element is the mean value of resisitivities obtained for all independent excitations. The obtained images can be filtered in order to reach a better quality, but resolution in the centre is poor. The different modifications of this method called backprojection can be found in literature [5,6].

2° — Perturbation method

In this method a perturbation matrix i.e. dependence of the change in measured current or voltage as a function of the change in resistivity distribution is used [7]. In each iteration the new value of resistivity is calculated and then the perturbation matrix is modified. The resistivity is calculated from the formula:

$$\rho_i^n = \rho_i^{n-1} + k \frac{\sum_{j=1}^{J} C_{jl}^n T_{ijl} \rho_i^{n-1}}{\sum_{j=1}^{J} |T_{ijl}|},$$

where ρ_i^n, ρ_i^{n-1} resistivity of element i-th after n, $(n-1)$ correction respectively, k — overrelaxation coefficient, T_{ijl} — perturbation matrix for i-th element and j-th

current measurement in the l-th projection angle, C_{jl}^{n} — percent difference between the predicted and actual current density magnitudes at the current-sensing electrode j for l-th projection angle at the n-th correction. In Kim [7] method (sometimes called ART — algebraic reconstruction technique) the perturbation matrix is calculated only once. Yorkey [8] has showed that perturbation matrix is a function of resistivity distribution, so it should be calculated after each iteration. The formula used is of the form:

$$\rho_i^n = \rho_i^{n-1} + k \frac{\sum_{l=1}^{L} \sum_{j=1}^{J} C_{jl}^{n} T_{ijl} \rho_i^{n-1}}{\sum_{l=1}^{L} \sum_{k=1}^{J} |T_{ikl}|}.$$

This technique is similar to SIRT (Simultaneous Iterative Reconstruction Technique). These modifications cause that algorithm is more stable for conductivity changes near the surface, but they increase the reconstruction time.

3° — Sensitivity method

This is an iterative method based on Geselowitz theorem [9,10]. The impedance changes caused by the conductivity changes can be calculated from the formula:

$$\Delta Z = -\int_V \Delta\sigma \frac{\nabla \phi}{I_\phi} \bullet \frac{\nabla \varphi}{I_\varphi} dV,$$

where: ϕ — the potential distribution associated with the I_ϕ current flowing between „current" electrodes, φ— the potential distribution associated with hypothetical I_φ current flowing between „voltage" electrodes after the conductivity change $\Delta\sigma$ occurrence, „•"— the scalar product. The function

$$S = -\int_V \frac{\nabla \phi}{I_\phi} \bullet \frac{\nabla \varphi}{I_\varphi} dV$$

is called sensitivity. If it is assumed that the value of conductivity is constant in each element (obtained after the discretization) then the impedance changes for each measurement port are equal to:

$$\Delta Z_i = \sum_j \Delta\sigma_\varphi S_{ij}.$$

From the above formula the conductivity change can be calculated and then new value of conductivity is obtained. The main problem in using this method is, in some application, time needed to inverse sensitivity matrix. This matrix is ill-conditioning and large numerical errors during inversion can appear. Another method to solve this equation is to use itereative tehnique (it is no necessary to calculate inverse matrix), but it is also time consuming.

4° — Gauss-Newton method

This method [4] is based on minimisation of the following functional:

$$\Psi(\rho) = (v(\rho) - u)^T (v(\rho) - u),$$

where: ρ — resistivity, v — calculated potential vector for prescribed resistivity ρ, u – measured potential. The resistivity changes can be obtained from the formula:

$$\Delta\rho^{(i)} = -\left(\left(\frac{\partial v}{\partial \rho^{(i)}}\right)^T \left(\frac{\partial v}{\partial \rho^{(i)}}\right)\right)^{-1} \left(\frac{\partial v}{\partial \rho^{(i)}}\right)^T \left(v(\rho^{(i)}) - u\right)$$

The advantage of this method is very fast convergence (the error diminishes with power two) to the minimum of the functional i.e. real value of resistivity. The main drawback of this method is small region of convergence i.e. if assumed, in first iteration, resistivity distribution is far from the real one, the algorithm can lead to „false positive" images or convergence can not be reached.

5° — Wexler double-constraint algorithm [11,12]

Let us consider differential equation

$$\nabla \cdot (\sigma \nabla \phi_1) = 0 \text{ in } \Omega,$$

where Ω is the examined object, with boundary conditions

$$\sigma \frac{\partial \phi_1}{\partial n} = 0 \text{ on } \Gamma_e,$$

$$\sigma \frac{\partial \phi_1}{\partial n} = I \text{ and } \int_{\Gamma} \phi dS = \text{on } \Gamma - \Gamma_e.$$

The second equation

$$\nabla \cdot (\sigma \nabla \phi_2) = 0 \text{ in } \Omega$$

and boundary conditions

$$\sigma \frac{\partial \phi_2}{\partial n} = 0 \text{ on } \Gamma_e,$$

$$\phi_2 = \phi_\mu \text{ on } \Gamma - \Gamma_e,$$

where:

ϕ_m — measured potential, I — injected current, Γ_e — pair of injection electrodes.

For true conductivity value $\phi_1=\phi_2$. If these potentials are not equal, the functional Ψ of mean square deviation between current distributions in Ω corresponding to these potentials can be defined as follows:

$$\Psi(\sigma) = \sum_{injections} \sum_{i} \int_{\Omega_i} \| \sigma_i \nabla \phi_2 - \sigma_i \nabla \phi_1 \|^2 \delta \Omega_i ,$$

where σ_i is a conductivity of i-th element Ω_i. After minimalisation the new value of conductivity σ_i' is obtained

$$\sigma_i' = \frac{\sum_{injections} \int_{\Omega_i} - \sigma_i \nabla \phi_1 \nabla \phi_2 d\Omega_i}{\sum_{injections} \int_{\Omega_i} \| \nabla \phi_2 \|^2 d\Omega_i} .$$

This method is unstable and an increase in the number of iterations does not improve satisfactorily the quality of images.

6° — *Optimal control algorithm [13]*

It is based on linearization of the following equation

$$\nabla \cdot (\sigma \nabla \phi) = 0.$$

Let $\sigma = \sigma^{(0)} + \Delta\sigma$, $\phi = \phi^{(0)} + \Delta\phi$, where $\phi^{(0)}$ is potential distribution for assumed conductivity distribution $\sigma^{(0)}$. With these assumptions (1) is as follows

$$\nabla(\sigma^{(0)} \nabla \phi^{(0)}) + \nabla(\sigma^{(0)} \nabla \Delta\phi) + \nabla(\Delta\sigma \nabla \phi^{(0)}) + \nabla(\Delta\sigma \nabla \Delta\phi) = 0. \quad (1)$$

And from this

$$\nabla(\sigma^{(0)} \nabla \Delta\phi) \approx -\nabla(\Delta\sigma \nabla \phi^{(0)}). \quad (2)$$

Now it is possible to calculate $\Delta\sigma$ by minimising the functional

$$\Psi(\Delta\sigma) = \frac{1}{2} \sum_{l=1}^{L} \sum_{k=1}^{K} \left(\Delta \underline{v}_k^l (\Delta\sigma) - \Delta \underline{\phi}_k \right)^2 + \frac{\mu}{2} \int_{\Omega} |\Delta\sigma|^2 dV,$$

where: $\Delta \underline{\phi}_k$ — difference between measured and calculated potential for k-th measurement and l-th stimulation, $\Delta \underline{v}_k^l$ — difference between potential with conductivity distribution $\Delta\sigma$ and previous for k-th measurement and l-th stimulation, μ — regularization parameter.

After simple calculations and with use of FEM the functional

$$\Psi(\Delta\sigma) = \frac{1}{2} \sum_{l=1}^{L} \Delta \underline{v}^{l\,T} \Delta \underline{v}^l + \frac{\mu}{2} \Delta\sigma^T Q \Delta\sigma - \sum_{l=1}^{L} \Delta \underline{\phi}^{l\,T} \Delta \underline{v}^l \quad (3$$

is obtained, where Q is diagonal matrix of volumes of elements. Now (2) can be written as

$$\underset{1\le l\le L}{\forall} \quad \boldsymbol{A}\,\Delta\underline{v}^{l} = \boldsymbol{B}^{l}\Delta\sigma. \tag{4}$$

Calculating $\Delta\underline{v}^{l}$ from (4) equation (3) became

$$\Psi_1(\Delta\sigma) = \frac{1}{2}\,\Delta\sigma^{T}\boldsymbol{R}\,\Delta\sigma + \boldsymbol{c}^{T}\Delta\sigma,$$

where:

$$\boldsymbol{R} = \sum_{l=1}^{\Lambda} B^{l\,T}(A^{-1})^{T}A^{-1}B^{l} + \mu Q,$$

$$\boldsymbol{c} = -\sum_{l=1}^{\Lambda} \boldsymbol{B}^{l\,T}(\boldsymbol{A}^{-1})^{T}\Delta\phi.$$

Finally after minimisation

$$\Delta\sigma = \boldsymbol{R}^{-1}\boldsymbol{c}.$$

The main drawback of this algorithm is high acceleration of measurement errors. Another problem is reconstruction time, but it can be reduced as was shown in [14].

Other groups of methods are based on neural networks or genetic algorithms [15,16] but these types of algorithms are not considered in this work, as the possibility to use these methods to solve the 3D problem is not proved, yet.

3. Algebraic reconstruction technique with regulated correction frequency (RCFART) [2]

The quality of images obtained by presented reconstruction techniques are similar. These algorithms differ in memory consumption and computation complexity, which affected the time needed to obtain the reconstructed image. M. Kocikowski [2] proposed as a base for further modification the perturbation method because it was faster than others. He proposed a generalised algorithm with regulated correction frequency:

$$\sigma_e^{(h+1,i)} = \sigma_e^{(hi)} + k\,\sigma_e^{(hi)}\,\frac{\sum_{j=1}^{L/H}\sum_{k=1}^{K} c_k^{(li)} s_{p(k,l)e}^{(i)}}{\sum_{j=1}^{L/H}\sum_{k=1}^{K}\left|s_{p(k,l)e}^{(i)}\right|},$$

$$\sigma_e^{(1,i+1)} = \sigma_e^{(H+1,i)}.$$

For prescribed iteration i in succeeding corrections h $(h=1...H)$ the σ_e (conductivity of elements) are modified for subset of L/H uniform spread excitations l.

Corrections are proportional to the current value of conductivity — $\sigma_e^{(hi)}$, normalised covariance of relative changes k-th currents measured to calculated for l-th excitation — $c_k^{(li)}$ and sensitivity for element e - $s_{p(kl)e}^{(i)}$. The correction frequency H should be equal to L/N, where N is a natural number. To speed up the reconstruction process modification of overrelaxation coefficient was introduced. The proposed modification of overrelaxation constant k makes it dependent on the distance from the surface:

$$k(d) = 1 + (k_{max} - 1)\frac{d}{R},$$

where: d is the distance of the centre of an element from the surface, R — the radius of hemisphere. Such modification of overrelaxation coefficient was possible because of special dedication of this algorithm to mammograph with hemispherical measurement chamber. Such definition of k can increase the sensitivity for the contrast and resolution inside the examined object without generating big errors near the surface. It allows greater modifications of conductivity in the central region, when sensitivity is low and smaller one near the surface, where sensitivity is big.

Some effort was put on minimalization of memory requirements for reconstruction process. The sensitivity matrix is calculated each time it is needed, so consumption of memory is substantially reduced.

4. Models of electrodes and complexity of calculations

In a reconstruction process appropriate division of a model of examined object into elements is important. The number of different reconstructed values of conductivity (different separated regions) must be equal or lower than the number of linearly independent measurements. From that, if there is no apriori knowledge of conductivity distribution in the examined region, the uniform mesh should be used. On the other hand most elements should be placed near the exciting electrodes. This is due to the biggest potential distribution changes in this region. Also low resolution in the centre of the examined object causes that there is no necessity to put many elements in that region.

An important problem is also the model of electrode [17] used for forward (also used in reconstruction algorithms) and inverse problem, i.e. the assumed boundary conditions. The potential distribution is described by the following equation:

$$\nabla \cdot (\sigma \nabla \phi) = 0$$

where: ϕ — potential, σ — conductivity. It is assumed outside the electrodes that the normal flux of current vanishes, which has mathematical form as follows:

$$\frac{\partial \phi}{\partial n} = 0$$

The boundary condition on the remaining part of the surface depends on the assumed model of the electrode. One possibility of such condition is:

$$\sigma\frac{\partial\phi}{\partial n} = I/S_e \qquad \text{and} \qquad f\sigma\frac{\partial\phi}{\partial n} = -I/S_e$$

where S_e - area of electrode. For metal electrodes one can assume that the whole electrode has the same value of potential:

$$\phi_e = \phi,$$
$$I = \int_{S_e} \sigma\frac{\partial\phi}{\partial n}ds.$$

In models which take into account also the impedance of electrode layer the following equation should be used

$$\phi + z_e\,\sigma_e\frac{\partial\phi}{\partial n} = \phi_e,$$

where: σ_e — conductivity of electrode layer, z_e — impedance of electrode layer. It is also possible to put some additional elements for electrode and modify their conductivity to suit the electrode for better simulation result.

In the first two cases there are no additional non zero elements in the matrix equation used to solve the forward problem (obtained using FEM), i.e. to find potential distibution in the examined object. The difference will be in number of nodal voltages which have to be calculated. In the case of metal electrode with assumed potential on its surface the calculation cost will be lower (less nodal voltages to calculate). In the case of taking into account the impedance of electrode layer the modification of matrix is necessary (additional cost for calculation elements of matrix). The last case with additional elements for electrode increases matrix dimension. From the above it is obvious that different boundary conditions cause different complexity of calculation (which is connected with different time consumption) and gives different potential distribution near an electrode.

To show the influence of computer (speed of processor and/or available memory) used for reconstruction some comparison of different computers was done. Table* below shows the time needed for reconstruction of a hemisphere model with cylinder inside. The mesh consists of 3824 elements and 857 nodes. Results for 10 iterations are shown.

Procesor	***R10000 Power Challenge***	***R4400***	***Ultra-Sparc 167MHz***
time [min]	1.48	7.82	4.91

*The calculations were done on CI TASK computers.

5. Results

To check the proposed algorithm many simulations have been performed [2]. Models with different sizes of perturbed area, different locations and different values of perturbations were created. The influence of measurement noise, electrodes' impedances, number of measurement electrodes, assumed starting conductivity distribution, number of iteration needed to obtain good quality of reconstructed image were tested. Also the influence of value and modification (dependence on the distance from surface) of overrelaxation coefficient were tested. The number of correction used in algorithm was checked. Figures 1 to 4 show examples of models with two perturbations, assumed conductivity distribution and results of reconstruction procedure for 16 electrodes. Figure 5 shows an example of phantom reconstruction of an object with a volume 50 times smaller than the measurement chamber volume.

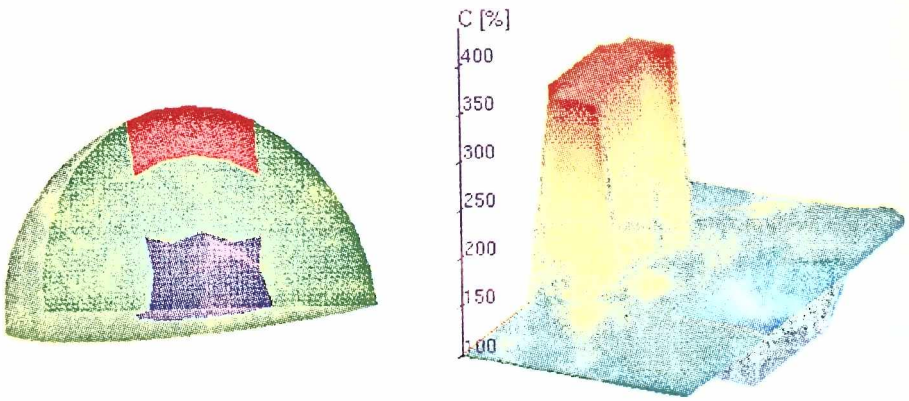

Figure 1. *Model and assumed conductivity distribution.*

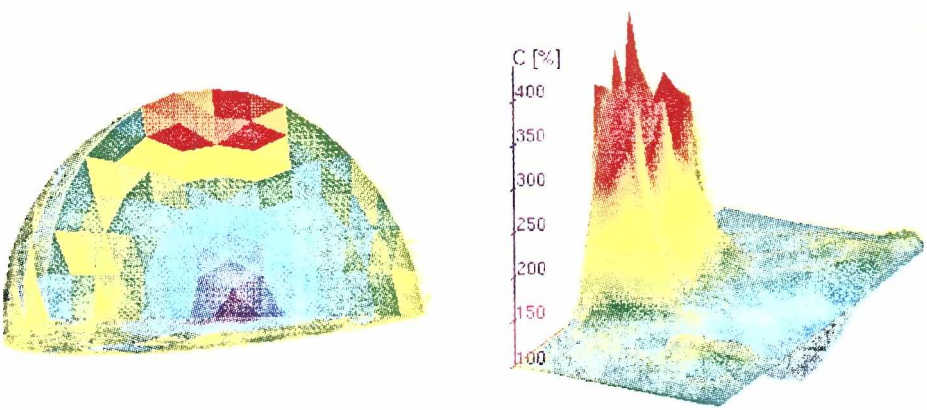

Figure 2. *Results of reconstruction of model from figure 1.*

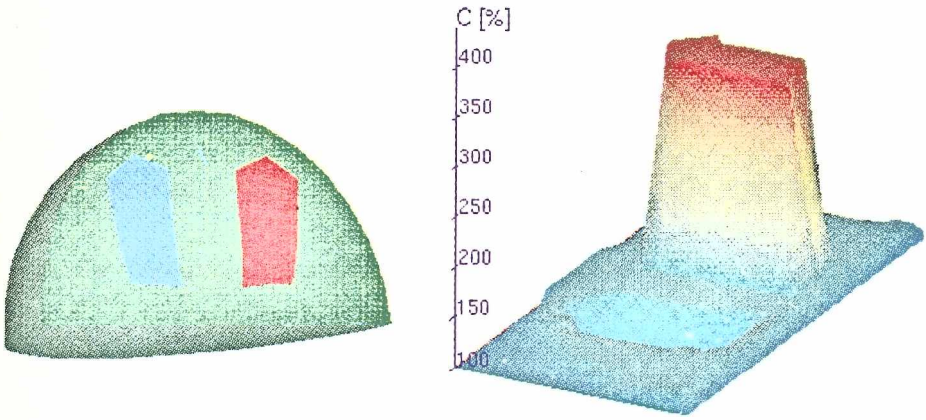

Figure 3. *Model and assumed conductivity distribution*

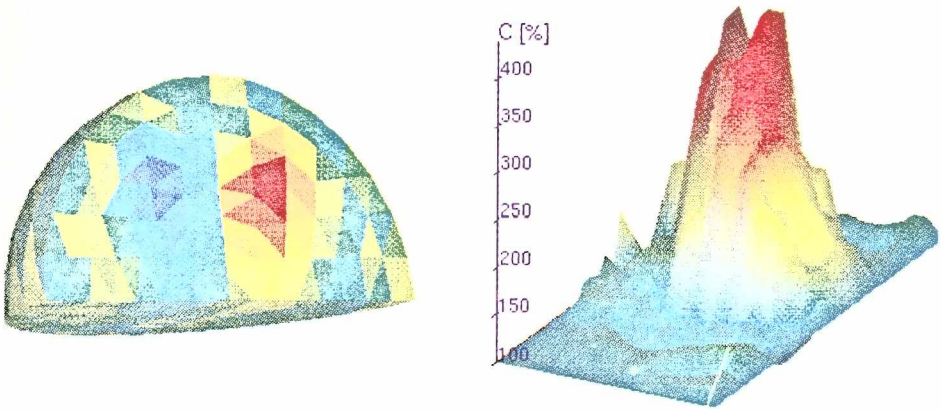

Figure 4. Results of reconstruction of model from figure 3

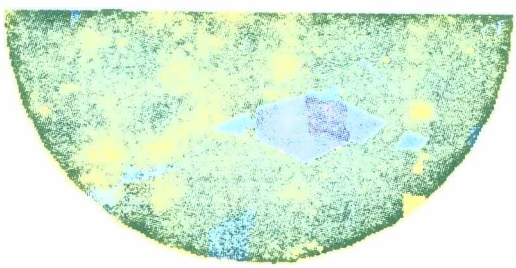

Figure 5. *Results of reconstruction of disk of 2% of volume of measurement chamber*

As it was expected the proposed algorithm (RCFART) has advantages of SIRT and ART algorithms avoiding some of their disadvantages. RCFART is much less sensitive than ART for perturbations near the surface (sensitivity is similar to SIRT) and has greater resolution than SIRT for perturbations in the centre of the examined object (similar to ART). The increase in the number of iterations increase the quality of obtained image (similar to SIRT). The algorithm is as fast as ART and as stable as SIRT.

6. Conclusions

The number of measurement electrodes should be increased to obtain better resolution and sensitivity in the centre of the examined object. Measurement errors should be small, to avoid amplifying them by reconstruction algorithm, which may result in a wrongly reconstructed conductivity distribution. Assumed conductivity distribution for the first iteration should be as close to the real one as possible (difference smaller than 50% is desirable). Reconstruction time of absolute value of conductivity distribution is still a problem for applications. One possibility to increase the speed is to use more elements in solving forward problem and less in inverse one (i. e. finding conductivity distribution in the examined object). Still new fast algorithms should be developed, as poor sensitivity and low resolution in the centre of the examined object is not fully solved. The table below shows approximate cost of one iteration for each method.

Algorithm	Approximate number of calculaitons
blackprojection	$2.8P^{1/2}E+0.285P^{1/2}E^{5/3}$
SIRT	$40EP+0.285^{1/2}E^{5/3}+0.015E^{7/3}$
sensitivity method	$13E^3$
Gauss-Newton method	$2E^2P+8E^{5/2}$
Wexler double-consistans method	$6EP+0.57P^{1/2}E^{5/3}$
optimal control algorithm	$4E^2+8EP$

Where: E — number of elements, P — number of independent measurements (P=(N-1)*N/2; N — number of electrodes).

Only multiplications and divisions were considered. It should be noted that different implementations have different calculation costs. There are also possible optimalizations. Not everything needs to be calculated in each iteration in each method. The methods differ also in the number of iterations needed to obtain satisfactory results of reconstruction.

References

[1] Proc. IX International Conference on bioimpedance, Heidelberg, Germany, 1995

[2] Kocikowski M., Reconstructin of 3-D images in EIT, PhD dissertation, Technical University of Gdansk, 1997

[3] Barber D. C., Brown B. H., Recent developments in applied potential tomography, Processing in Medical Imaging, ed. Bacharach, 106-1211, 1986

[4] Yorkey T. J., Webster J. G., Tompins W. J., Comparing reconstruction algorithms for electrical impedance tomograhy, IEEE-BME-34, 843-852, 1987

[5] Barber D. C., Brown B. H., Reconstruction of impedance images using filtred backprojection, Proc. of a meeting on EJT, Copenhagen 1990, pp. 1-8

[6] Barber D. C., Saeger A. D., Fast reconstruction of resistance images, Clin. Phys. Physical. Meas., vol. 8, sup. A, pp. 47-54, 1987

[7] Kim Y., WebsterJ. G., Tompins W. J., Electrical impedance imaging of the thorax, J. Microwave Power, vol. 18, 245-257, 1983

[8] Yorkey T. J., Webster J. G., Tompins W. J., An improved perturbation technique for electrical imaging with some criticism, IEEE-BME-34, 898-901, 1987

[9] Murai T., Kagawa Y., Electrical impedance computed tomography based on a finite element model, IEEE-BME-32, 177-184, 1985

[10] Geselowitz D. B., An application of electrocardiographic lead theory to impedance plethysmography, IEEE transactions on BME-18, 38-41, 1971

[11] Wexler A., Fry B. and Neiman M. R., Impedance-computed tomography algorithm and system, Appl. Opt. 24, 3985-3992, 1985

[12] Wexler A., Electrical impedance imaging in two and three dimensions, Clin. Phys. Physiol. Meas., 9 (Supp. A), 29-33, 1989

[13] Kozuoglu M., Leblebicioglu K., Ider Y. Z., A fast image reconstruction algorithm for electrical impedance tomography, Physiologigal Measurement, vol 15, A115-A124, 1994

[14] Sakamoto K., Kanai H., A fundamental study of an electrical imedance CT algorithm, Proc. V-th Int. Conf. Elect. Bio-Impedance, Zadar, Yugoslavia, pp. 349-352, 1983

[15] Cheng K-S et al, Electrical impedance image reconstruction using genetic algorithm, IEEE Conference, Amsterdam, 1996

[16] Adler A., et al, A neural network image reconstruction technique for electrical impedance tomography, IEEE Trans. Med. Imag., vol. 13 no.4, pp. 594-600, 1994

[17] Poliński A., Wtorek J., Nowakowski A., Modele elektrod w tomografii elektroimpedancyjnej, X Scientific Conference Biocybernetyka i Inżynieria Biomedyczna, vol. I, pp. 269-273, Warszawa, 1997

Reaserch financed by KBN grant 8T11E01710